1. Serafin Bachman[1] 2. Marek Turzyński[2] 3. Marek Jasiński[1]

Politechnika Warszawska, Instytut Sterowania i Elektroniki Przemysłowej (1)
Politechnika Gdańska, Katedra Energoelektroniki i Maszyn Elektrycznych (2)
ORCID: 1. 0000-0001-9589-7612;

Modern control strategy of bidirectional DAB converter with consideration of control nonlinearity

Abstract. This paper focuses on the control strategy for modern universal bidirectional Dual Active Bridge (DAB) converters for microgrid systems. An analysis of the converter equations was carried out, and typical problems related to the influence of dead time on the system operation were discussed. A closed control loop was developed, then tested by simulation and on a laboratory stand.

Streszczenie. W artykule omówiono strategię sterowania nowoczesnych uniwersalnych dwukierunkowych konwerterów Dual Active Bridge (DAB) dla systemów mikrosieci. Przeprowadzono analizę równań przekształtnika i omówiono typowe problemy związane z wpływem czasu jałowego na pracę układu. Opracowano zamkniętą pętlę sterowania, którą następnie przetestowano metodą symulacyjną i na stanowisku laboratoryjnym. (__Nowoczesna strategia sterowania dwukierunkowym konwerterem DAB z uwzględnieniem nieliniowości sterowania__).

Słowa kluczowe: DAB, projekt, optymalizacja, sterowanie.
Keywords: DAB, design, optimization, control.

Introduction

Microgrids are an important issue in the modern power industry. This concept involves combining AC and DC installations into a coherent whole system to adapt to the needs of various solutions in the field of electrical engineering developed worldwide. Technology applications include AC/DC/DC/AC converters used in renewable energy solutions; charging systems for intelligent energy storage; electric vehicle charging substations using hydrogen technology [1]; network systems using DC Bipolar installations [2]. Such a system's stability and operational reliability are essential to achieve the assumptions of electromobility, V2G (ang. Vehicle to Grid) [3]. The inability to control and disconnect system parts safely precludes these concepts. The current problems faced by all power systems include the development of the power grid, increasing the electricity demand, improving the quality of electricity, increasing the share of renewable energy sources in the energy market, and managing the expanding electricity network. The concept of a microgrid is to solve the problem and is currently being tested in research units all over the world.

This paper focuses on the proper control strategy for modern universal bidirectional Dual Active Bridge (DAB) converters tailored for microgrid systems. Anticipated is a positive trajectory towards advancing secure and eco-friendly power distribution within domestic and local microgrid systems. A study [1] underscores that DAB converters serve as pivotal elements in a well-balanced microgrid, owing to their bidirectional nature, isolation capabilities, efficiency, and power ratio. However, formulating an appropriate control strategy for bidirectional converters across a broad spectrum of applications is not a straightforward endeavor. The non-linear characteristic of DAB necessitates careful consideration in the design of magnetic components for diverse applications, involving an exploration of dead time effects and voltage drops across semiconductor elements.

This publication emphasizes the meticulous design of a control strategy for modern DAB converters. Furthermore, it delves into the intricacies of internal energy transfer, phase shift drift (a), changes in the polarity of AC output voltage, AC output voltage sag, non-symmetrical characteristics in zero phase shift (φ), positive power flow, and reactive energy flow in the drift time region. All presented information will be substantiated through subsequent simulation analyses and laboratory experiments.

Dual Active Bridge converter real application issues discussed in the paper

Fig. 1 represents a scheme of the classic design of one phase Dual Active Bridge (DAB) converter discussed in this paper.
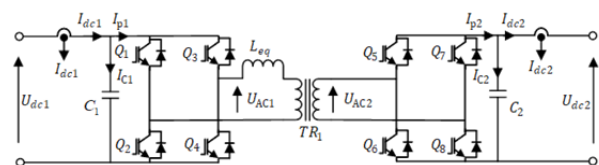

Fig.1. Dual Active Bridge (DAB) scheme.

The control strategy must address several challenges inherent in the standard Dual Active Bridge (DAB) topology, including internal energy transfer, phase shift drift, changes in the polarity of the AC output voltage, AC output voltage sag, non-symmetrical characteristics in zero phase shift, positive power flow, and reactive energy flow in the region around the dead time. These complexities make it difficult to determine precise characteristics and, consequently, impede the precise control of output power through phase

shift on the leakage inductance (L_{eq}). While prior publications, such as [5] - [9], have discussed these issues, there remains a gap in understanding the impact of real-world characteristics on the operation of DAB and fundamental control methods adapted to an ideal system.

An essential aspect of controlling DAB converters involves the modulator. Currently, the most prevalent and well-known modulator is the Single Phase Shift (SPS) modulator, renowned for its high efficiency in the state with a voltage ratio equal to one [10]. Another noteworthy control approach is Dual Phase Shift (DPS), a widely popular [11] method based on introducing a phase shift between the bridges, as illustrated in Fig 2. The Triple Phase Shift (TPS) represents the most intricate modulation method, extensively explored and studied in numerous publications, such as [12]. The Triple Phase Shift (TPS) modulation method is computationally intensive and requires a precise understanding of system parameters to determine the correct behavior of the Dual Active Bridge (DAB). While this method allows for a significant reduction in circulating current phenomena, its complexity makes it challenging to justify its application in scenarios that do not necessitate dynamic simultaneous changes in voltage, power, and energy flow direction.
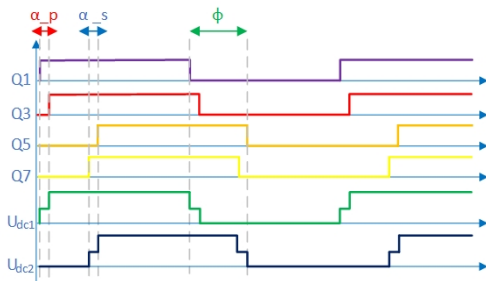
a)
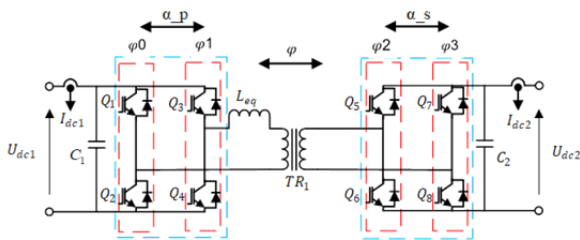
b)

Fig.2. DPS modulation concept. a) Phase shift distribution with basic φ phase shift and additional α_p and α_s shifts, b) voltage and current shapes for input and output side of magnetic components.

The issues of an experimental model of DAB in relation to an ideal theoretical model

The presented characteristics of DAB circuits in most publications are based on simplifying assumptions, omitting losses, and linearizing the characteristics. In a practical laboratory layout, however, it is impossible to ignore such aspects as, for example, dead time DT. The dead time ensures the safe operation of the converter by not shorting the keys in the branches, and its value depends on the hardware capabilities, the possible resolution of the PWM (pulse width modulation) signal of the control system, as well as the characteristics of the selected transistor, switching frequency, etc. In modern designs, it can be assumed the simplification that the optimal dead time is in the range of 1-2% of switching period time. The simplified equation adopted in this publication based on [6] – [9] is presented.

The dead time in DAB converters is responsible for two fundamental issues: the initial shape of the DAB power characteristic for a phase shift less than or equal to twice the dead time; and the soft-switching characteristics for transistors.

The first dependence of the characteristic can be calculated based on the drift coefficient [6]:
Definition of dead time drift effect [6]:

(1) $a = \frac{2T_{DT}}{T_{SW}} \ for \ k_u > 1 \ and \ a = \frac{-2T_{DT}}{T_{SW}} \ for \ k_u < 1$

(2) $a = \frac{\varphi_{DT}}{\pi}$

Passive power transfer condition:

(3) $\qquad |\varphi| < a$

where T_{DT} is the dead time; T_{SW} is the switching period; k_u is the voltage ratio of the secondary side voltage U_{dc2} to the primary side voltage U_{dc1} (considering the transformer voltage ratio n). The voltage ratio of the output to the input is controlled by a given phase shift. This factor indicates the direction of power flow, the value of the phase shift is controlled by means of φ angle. The *a* parameter form equations 1 -3, means drift time.

Equation 3 specifies that the phase shift setpoint should be greater than the drift value. This dependence applies to the positive and negative parts of the characteristic.

The drift duration factor describes the inactive operating state of the DAB. In the DAB there is no active switching cycle for phase shift states in the drift range. Diode conduction occurs when transistor conduction is expected according to an ideal characteristic. This phenomenon occurs strongly at a low value of the output current as presented in [6].. This phenomenon causes the occurrence of reverse current with additional reactive power, distortion of the output voltage, change of the phase voltage polarization, and other problems [7].

Another important parameter influenced by the dead time change is the soft-switching range of the transistors. According to the exemplary characteristic drawn for the tested DAB system, as presented in Fig. 3.
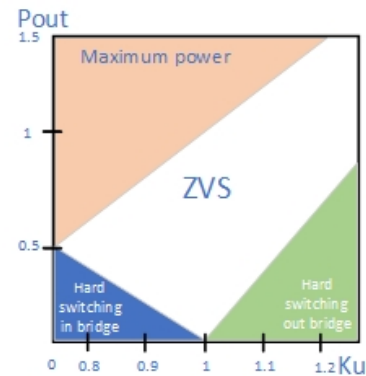

Fig.3. Zero Voltage Switching (ZVS) region characteristic with presented ideal transistor soft-switching characteristic.

The possibility of soft-switching of transistors is an important advantage of DAB converters and can be seen in Fig. 3, it is possible in a wide voltage range. Providing ZVS is important because it allows for reducing the switching losses of transistors. The state of soft-switching is strongly correlated with the operating frequency and the voltage ratio of the system. The ZVS condition for the DAB converter is presented below and discussed thoroughly in [6]:

(4) $\varphi > \frac{\left(1 - \frac{1}{k_u}\right)\pi}{2}$ and $\varphi > \frac{(1-k_u)\pi}{2}$

This phenomenon strongly influences the characteristic shown in Fig. 3 above, since the transistor key soft-switching phenomenon occurs by switching the transistor in the zero-voltage switching. This is preceded by the discharge of the transistor's own capacity during the dead time, the discharge current characteristic is limited by the resultant inductance of the converter. Holdoff time is the time resulting from the duration of dead time and corresponds with the time when the capacitance of the transistor is being discharged. This means that decreasing the holdoff time can reduce the soft switching region and increasing the holdoff can cause additional switching losses and a decrease in system efficiency. A simplified equation for determining the value of the discharge current of the transistor capacitance for ZVS:

(5) $I_{cs} = 2C_s * \frac{dV_{cs}}{dt}$

The I_{cs} is the nominal discharge current of the semiconductor, C_s represents the total capacitance of semiconductor between drain and source pin, V_{cs} represents the voltage across the transistor.

Discharging the capacitance causes the voltage to drop across a given connector so that it is possible to start conduction through a diode in the structure of the transistor. The diode activation begins at a specific value of the threshold voltage resulting from the diode characteristics. Then the transistor is turned on. Procedure is presented on Fig.4. and example soft switching characteristics is presented on Fig. 5.
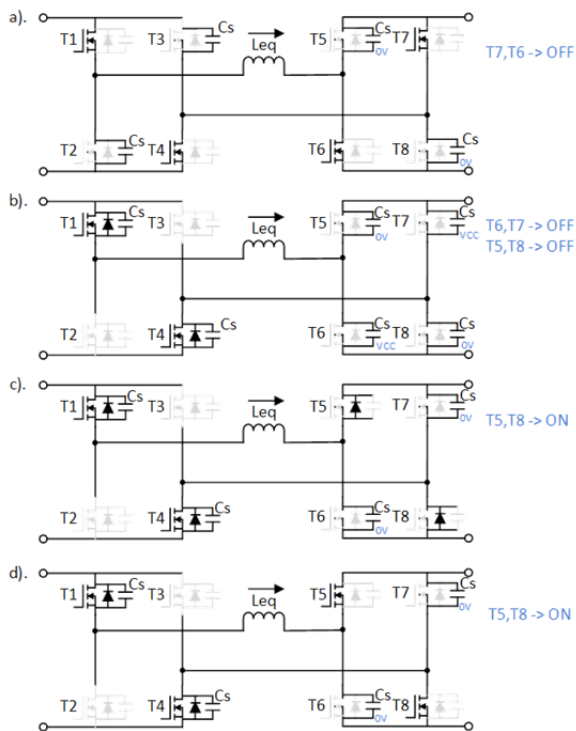

Fig.4. ZVS switching process example. A) Switching OFF T7, T6, b) All keys of secondary side switched off, c) Switch ON T5, T8 by internal Diode, d) Transistors switched ON.

Additionally, switching losses of transistors should be added to the phenomena distorting the ideal characteristics of DAB. MOSFET transistor (metal-oxide-semiconductor field-effect transistor) consists of the internal diode and

transistor structure. Their unfavorable influence on switching losses and voltage drop cause further distortion of the DAB converter characteristics. Losses of conductive elements are strongly correlated with the operating temperature of the silicon structure and humidity. It means that can be vary depends on the working environment. The losses cannot be neglectable for low voltage solutions.
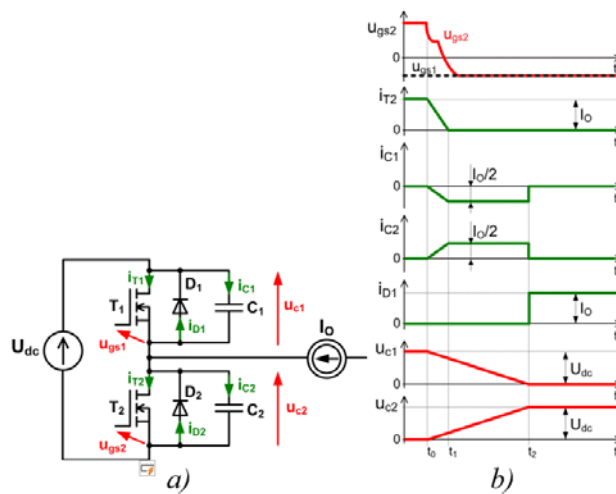

Fig.5. Soft – switching in a half – bridge circuit: a) scheme, b) theoretical waveforms during transistor T$_2$ turn-off at ZVS conditions.

Taken together, all these phenomena mean that the ideal shape close to the linear characteristic cannot be kept. Fig. 6, shows a comparison of the ideal character with an exemplary characteristic obtained from simulation testing of the DAB. The simulation tests were carried out for a switching frequency of 50kHz, leakage inductance of 67uH, magnetization inductance of 3mH, nominal power of 10kW for 0.15 p.u phase shift. Voltage ratio 1.82. Primary voltage 690V and secondary voltage 380V.
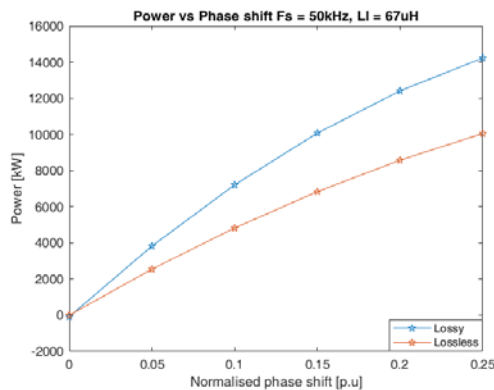

Fig.6. Ideal vs non-ideal DAB characteristic example.

Based on these results, it can be seen that the DAB simulation without taking into account the dead time will introduce a significant error in the output power value at a given phase shift. This can cause a difference between the laboratory setup and the simulation, including a difference in the settings of the PI controllers. For this reason, it is recommended to take dead time into account when simulating the DAB topology. Dead time may not be included in the simulation to reduce execution time, but it is worth keeping in mind the issues discussed above.

It is worth noting that due to the change in characteristics, the principle of controlling the converter

should change. Depending on simulation requirements the non-ideal characteristic can change. In the case of Fig.5, the lossy characteristic has twice more transferred output power for a similar phase shift. It means that is necessary to simulate the DAB converter with dead time and transistor losses for proper inductance selection. It is also worth noticing that the characteristics of DAB are starting to be nonlinear after some point. Due to the pointed facts, we make assumptions for control strategies:

Excluding the work of the system in terms of the drift effect range of eq. 3. And limiting the maximum range of the phase shift to the value of $\pi/2$.

This limitation results from the assumption of control in the linear range of the characteristic. Controlling the system for phase shifts exceeding this value causes problems with instability of the PI controller operation and a total decrease in the efficiency of the system due to increased losses [10].

The control strategy synthesis

The main method of controlling the DAB converter is the method consisting of the phase shift between the phase voltages of the H bridges. Normalization of the phase shit is the method of scaling phase shift in per unit range. For the purposes of this work, we will use the normalized phase shift in the range of the per unit value <-0.5, 0.5> corresponding analogously to the range:

(6) $\quad < -\pi/2 \,; \pi/2 >$

(7) $\varphi = \pi * D => D = \frac{\pi}{\varphi}$

Simplified lossless equation of DAB phase shift [6]:

(8) $\varphi = \frac{\pi}{2}\left(1 - \sqrt{1 - \frac{8L_{eq}f_{SW}|P_{OUT}|}{nU_{dc1}U_{dc2}}}\right)$

In the case of a laboratory setup, it is necessary to derive the above equation into the control loop. Based on this phase shift equation, the output power and leakage inductance equations were created:

(9) $P_{OUT} = \frac{U_{dc1}U_{dc2}\varphi(\pi-\varphi)}{2\pi^2 f_{SW}L_{eq}}$

(10) $\quad L_{eq} = \frac{\frac{U_{dc1}U_{dc2}\varphi(\pi-\varphi)}{2\pi^2 f_{sw}}}{P_N}$

Based on the presented equations, the characteristics of the DAB converter system can be determined. The characteristics of the phase shift with respect to the power for a given frequency range and the characteristics of the power to the phase shift for various voltage ratio factors are shown in Fig. 7-8.
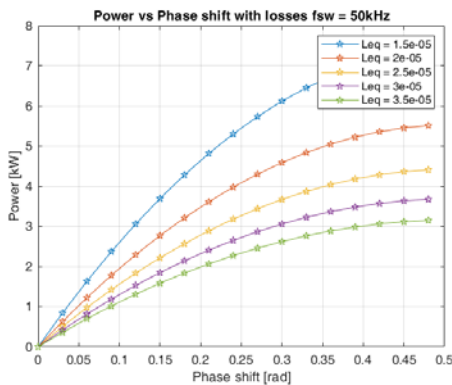

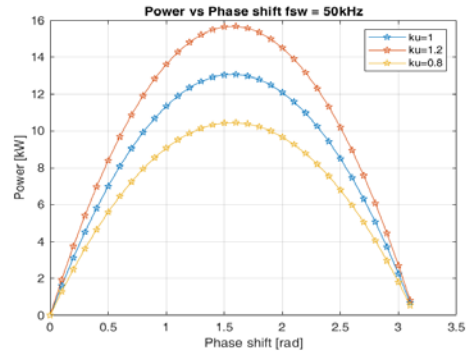Fig.7. Power to phase shift characteristic depends on L_{eq} inductance value.

Fig.8. Output power to phase shift characteristic with voltage ratio difference. Where k means k_u.

Based on above results, the following conclusions could be formulated: the range of switching frequency may result in the necessity to use additional serial magnetic components; when the system is limited by the value of the leakage inductance of the transformer, it is possible to change the power of the system by the switching frequency; the voltage transformer ratio may vary within a range of about 40% control the value of the output power at the maximum phase shift; the frequency and range of the voltage ratio determine the correct selection of the magnetic circuit of the DAB converter.

The DAB system regulation structure presented in Fig.9, based on the above assumptions, enables the safe operation of the system within the assumed phase shift. The presented control loop is based on SPS modulation with a soft start of the converter. The modulation works at a fixed 50% duty cycle. It is possible to operate the system as a regulator: current, voltage-current, power-current. The control loop allows you to adjust the control loop depending on the state, based on the converted values. The Min block deals with the selection of the appropriate value. The selected value of the set current then goes to the current regulator. The ability to change the control loop while the system is operating allows for greater flexibility in system control. Different types of DAB topologies can be driven by this method, for this purpose it is necessary to change the phase shift equation block and the modulator.
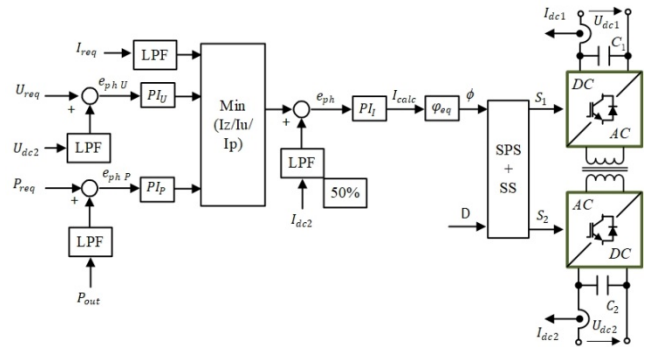

Fig.9. Control strategy for DAB converter

The Pi controller parameters calculation

In simplified form, the determination of the coefficients of the current regulator, assuming the ideal characteristic of the DAB, can be performed based on the equations:

(11) $\quad K_p = 1, \; T_i = \frac{T_s}{4*STC}$

Where T_s sampling time, STC sum of small-time constants, defined by the sum of $T_s + T_{PWM}$, where T_s is the time of the sampling period and T_{PWM} is the statistical delay of PWM generation. It is worth noting that in the case

of an ideal system, the entire converter gain is included in the phase shift equation, therefore it can be assumed that the gain is one. Unfortunately, when tuning the operation of the system on a laboratory stand, the non-ideal shape of the characteristic causes problems with set gain value. For proper controller settings, the low pass filter is necessary. Due to this fact it is required to use additional methods of linearization, dead time compensation, or manual tuning using the engineering method in a given operating range of the system.

Due to the nature of the operation, the circuit of the DAB converter with a current regulator, in the no-load, will cause a large error of the current value. The current controller will be forced to over-regulate the response to the limit value by the upper saturation limit. This phenomenon may cause a safety hazard due to the possibility of the exceeding voltage range of the secondary side. For this reason, it becomes necessary to implement additional voltage feedback in more demanding systems. This can be done by means of an active current limit of the computed current regulator. It is also possible to use an additional voltage and/or power PI regulator.

In the case of the considered circuit, a minimum value selection block was used, depending on the actual calculated setpoint by the voltage and power controller and the filtered value of the set current. With this solution, it is possible to test the operation of the system at many different operating points. Calculation of the voltage regulator settings can be performed based on [10] – [12]. Filter time constant is defined as it follows:

$$(11) \qquad T_f = \frac{2*\sqrt{\sqrt{2}-1}}{2\pi*30} = 6.82 * 10e^{-3}$$

Filter gain:

$$(12) \qquad K_f = \frac{2T_s}{T_f}$$

Sum of small time constant:

$$(13) \qquad STC = 1.5T_s + T_f$$

Proportional gain of PI controller::

$$(14) \qquad K_p = \frac{C_{dc}}{2*STC}$$

Time constant of PI controller:

$$(15) \qquad T_i = \frac{T_s}{4*STC}$$

It is worth paying attention to the values of the time constants of the current regulator, this system is significantly limited by the L / C time constant of the converter. Therefore, the dynamics of the DAB current control (~1ms) is much longer than typical active AC/DC converter.

The measured DC current taken as feedback control loop current is performed after the capacitive filter for this solution. This measurement method is limiting the problem with measuring and controlling the pulse current.

Laboratory verification compared to simulation results
The control strategy was implemented in a laboratory setup where the confirmation of the results was obtained. The presented results were compared with the simulation tests of the system in the PLECS program. Parameters of the laboratory stand:

The DSP + FPGA platform developed at IWUT was used to control the converter. The following equipment's were used for the tests: ITECH IT6018B laboratory power supply/load; Tektronix TCP0150 current probe and THD0100 voltage probes were used for the measurements.

Table 1. DAB Parameters

Primary voltage	670V
Secondary voltage	670V
Nominal power	10kW
Switching frequency	50kHz
Transformer core	3C95 ferrite core (SMA)
Turn ratio	1:1
L_{eq}	25 µH
Main inductance	503 µH

The results were collected on the basis of the setup diagram shown in Fig. 10 and11.
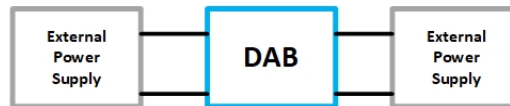

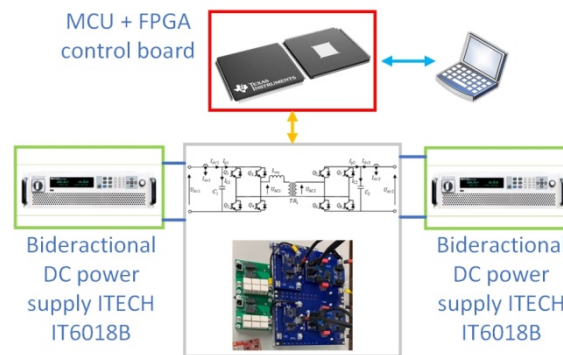Fig.10. Schematic of the laboratory setup.

Fig.11. Photo of the laboratory setup.

The results presented in Fig. 13 include an overshoot of the phase voltage due to the dead time drift effect. The value of the given offset is not much smaller than the value of the drift. In the case of Fig. 14, the value of the phase shift is equal to zero, which makes this effect more visible. This problem means that there is a phenomenon in which, due to the small voltage difference U_{dc1} and U_{dc2}, the series inductance current reaches a value close to zero. This is due to the occurrence of dead time between transistors. For this reason, there is an additional state in which all power is conducted by the diodes, and the transistors are turned off until the switching pulse appears. The solution to this problem is the correct selection of the series inductance and DT values.

In dynamic states, after changing the voltage (Fig. 15 – 16), the system stabilizes in the range of 100-20 ms, depending on the selected settings of the low pass filter of the set value. In Fig. 16, an additional overshoot of the magnetic current can be observed, this is caused by the delta change of the phase shift, causing a voltage difference across the series inductance, forcing the transformer to high current, its saturation and the appearance of a DC bias of the phase current. This phenomenon is known in the literature as L/R transient state. Preventing this phenomenon will be discussed in another publication

Fig. 17 shows the results with correctly designed parameters of the system based on the equations presented in this publication. This solution allows 100% to exclude problems related to dead time drift. This result can be compared to Fig.12.
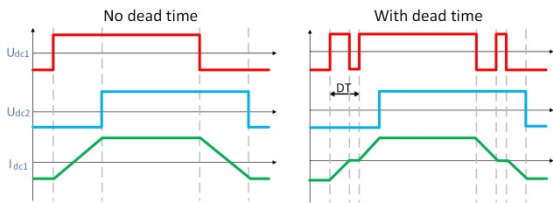
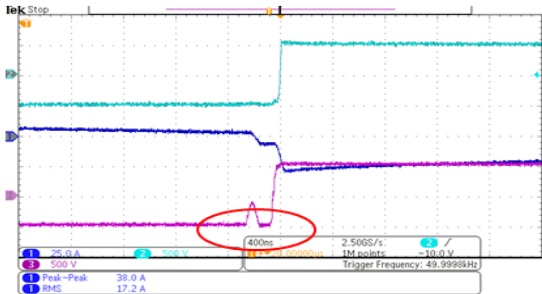Fig.12. Simulation results of dead time drift problem

Fig.13. DAB steady state problem with DT. CH3 purple – input DC voltage, CH1 blue – output DC voltage, CH2 cyan – inductor voltage, CH4 green – inductor current. The scale of the oscillogram time axis is 400ns.
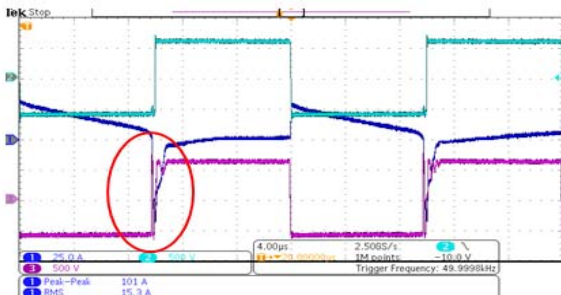

Fig.14. DAB steady state problem with DT. CH3 purple – input DC voltage, CH1 blue – output DC voltage, CH2 cyan – inductor voltage, CH4 green – inductor current. The scale of the oscillogram time axis is 400ns.
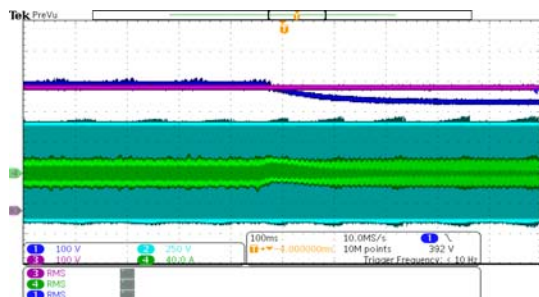

Fig.15. Transient in respect to the output voltage change from 400V to 360V, CH3 purple – input DC voltage, CH1 blue – output DC voltage, CH2 cyan – inductor voltage, CH4 green – inductor current. The scale of the oscillogram time axis is 100ms.
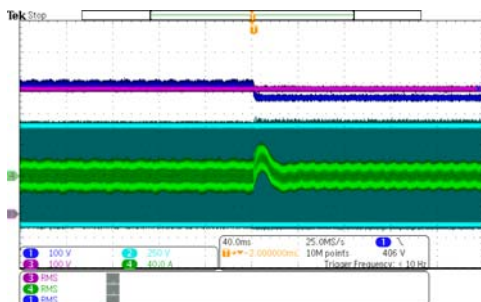

Fig.16. Transient in respect to the output voltage change from 400V to 360V with faster response, CH3 purple – input DC voltage, CH1 blue – output DC voltage, CH2 cyan – inductor voltage, CH4 green – inductor current. The scale of the oscillogram time axis is 40ms.

Load change tests of 50% were conducted and are depicted in Figs. 18-19, along with dynamic voltage variations in the range of 380V-340V. The results presented affirm the proper functioning of the system. In Fig. 20, a laboratory power supply was employed as a DC/AC load. The dynamics of voltage changes primarily result from the utilized power source and the load in the form of laboratory power supplies. Through the implementation of an appropriate converter design strategy and modulation method, it becomes feasible to eliminate the phenomenon illustrated in Fig. 13-14. Furthermore, the elimination of the dead time drift phenomenon was achieved by increasing the inductance value, which resulted in an enlarged control step beyond the range of hazardous phase shift.
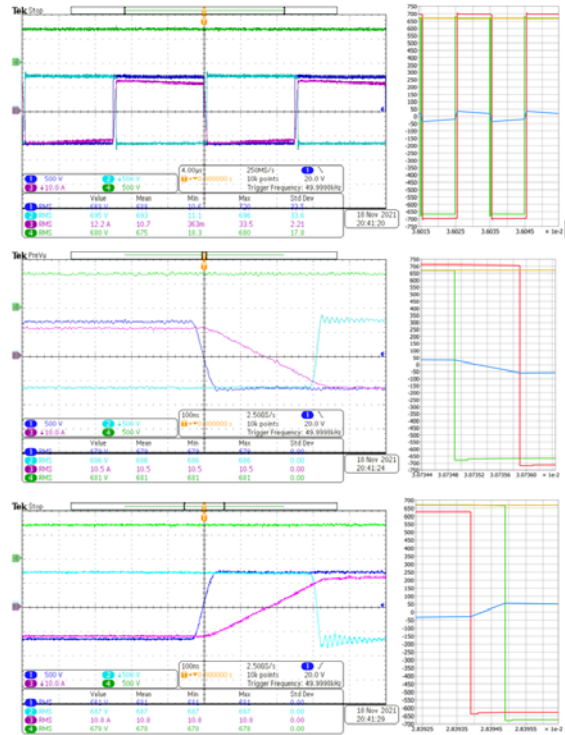

Fig.17. Steady state results. From TOP, general view, falling e``dge and rising edge. Channel 1 – Input voltage, channel 2 – output phase voltage, Channel 3 – inductor current, channel 4 – output DC voltage. On the left simulation results red- primary AC voltage, green- secondary AC voltage, blue – inductor current, orange – input DC voltage - The figure also shows the oscillations resulting from disturbances on the measurement court. They do not affect the operation of the system. The scale of the oscillogram time axis from top is 4us and 100ns.
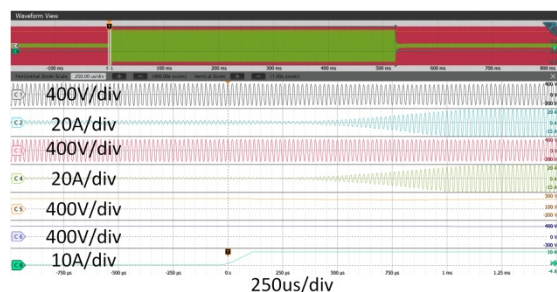

Fig.18. Dynamic load change step up. From top: C1 – primary side phase voltage, C2 primary side phase current, C3- secondary side phase voltage, C4 – secondary side phase current, C5 – input DC voltage, C6 – output DC voltage, C7 – output DC current.
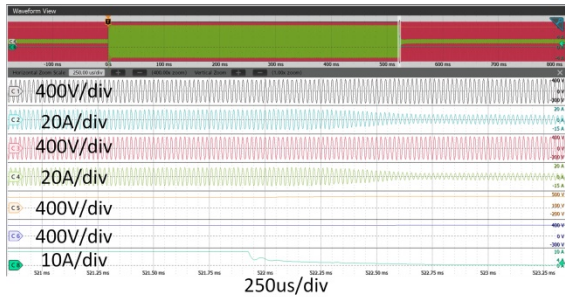
Fig.19. Dynamic load change step down. From top: C1 – primary side phase voltage, C2 primary side phase current, C3- secondary side phase voltage, C4 – secondary side phase current, C5 – input DC voltage, C6 – output DC voltage, C7 – output DC current.
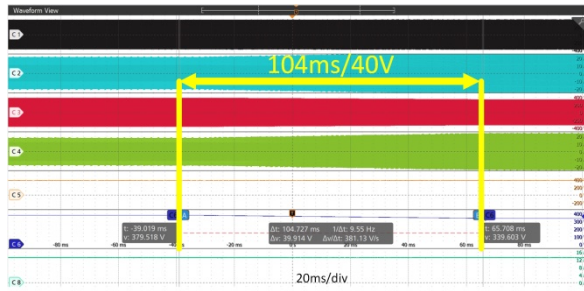

Fig.20. Dynamic voltage change from 380V to 340V with DC/AC load. C1 – primary side phase voltage, C2 primary side phase current, C3- secondary side phase voltage, C4 – secondary side phase current, C5 – input DC voltage, C6 – output DC voltage, C8 – output DC current.

Conclusions

The presented work delves into the selection of the control loop for the Dual Active Bridge (DAB) converter. The synthesis carried out was validated through both simulation modeling and laboratory experimentation.

The study addresses the challenge of determining the characteristics of a DAB-type circuit. Distortion of the power characteristic in relation to the phase shift of the DAB converter system arises due to various factors, including dead time, voltage ratio, voltage drops on the transistor and diode, and the soft-switching region. Significant distortion is observed within the drift phenomenon range, characterized by an inactive operating region and diode conduction.

A control method for the system, accounting for limitations arising from the non-ideal characteristics of the system, was presented and developed based on the DAB converter equations. The work also introduces methods for calculating the phase shift, as well as setting values for the current and voltage regulators.

In subsequent stages of the research, a comparison between simulation and laboratory results for the proposed DAB converter control structure will be further developed. The consistency between the presented laboratory results and simulation outcomes attests to the accurate implementation of the control structure.

Future work will concentrate on refining the control method and addressing starting problems. Subsequent research stages will involve a thorough examination of the control system at various voltage levels and with variable voltage ratios.

REFERENCES

[1]   N. Bazmohammadi et al., "Microgrid Digital Twins: Concepts, Applications, and Future Trends," in IEEE Access, vol. 10, pp. 2284-2302, 2022, doi: 10.1109/ACCESS.2021.3138990.
[2]   N. Bouisalmane et al., "Hydrogen consumption minimization with optimal power allocation of multi-stack fuel cell system using particle swarm optimization," 2021 IEEE Transportation Electrification Conference & Expo (ITEC), 2021, pp. 154-160, doi: 10.1109/ITEC51675.2021.9490111.
[3]   Xi Chen, Haihui Wang, Fan Wu, Yujie Wu, Marta C. Gonzalez, and Junshan Zhang. Multi-microgrids load balancing through ev charging networks. IEEE Internet of Things Journal, pages 1–1, 2021.
[4]   Sourav Das, Parimal Acharjee, and Aniruddha Bhattacharya. Charging scheduling of electric vehicle incorporating grid-to-vehicle and vehicle-to-grid technology considering in smart grid. IEEE Transactions on Industry Applications, 57(2):1688–1702, 2021.
[5]   C. Yang, H. Jin, H. Li, L. Yu, Y. Pei and L. Wang, "A Minimum Power Circulating Flow and Optimal Deadtime Control Method for GaN Based DAB Converter with EPS Control," 2021 IEEE 1st International Power Electronics and Application Symposium (PEAS), 2021, pp. 1-5, doi: 10.1109/PEAS53589.2021.9628802.
[6]   R. Barlik, M. Nowak, P. Grzejszczak. Power transfer analysis in a single phase dual active bridge, BULLETIN OF THE POLISH ACADEMY OF SCIENCES TECHNICAL SCIENCES, Vol. 61, No. 4, 2013 DOI: 10.2478/bpasts-2013-0088
[7]   J. Itoh, K. Kawauchi and H. Watanabe, "Non-linear Deadtime Error Compensation Method of Dual Active Bridge DC-DC Converter for Variable DC-bus Voltage," 2018 International Conference on Smart Grid (icSmartGrid), 2018, pp. 208-213, doi: 10.1109/ISGWCP.2018.8634560.
[8]   J. -I. Itoh, K. Kawauchi and H. Higa, "Deadtime Compensation with DC Offset Current Elimination Method Using Three-Level Operation for Dual Active Bridge DC-DC Converter," 2018 IEEE Energy Conversion Congress and Exposition (ECCE), 2018, pp. 6299-6306, doi: 10.1109/ECCE.2018.8557377.
[9]   S. Maharana, S. Mukherjee, D. De and A. Castellazzi, "Deadtime Compensated Dual Active Bridge with Online Hybrid Optimized Operation," 2021 1st International Conference on Power Electronics and Energy (ICPEE), 2021, pp. 1-6, doi: 10.1109/ICPEE50452.2021.9358608.
[10] B. M. Kumar, A. Kumar, A. H. Bhat and P. Agarwal, "Comparative study of dual active bridge isolated DC to DC converter with single phase shift and dual phase shift control techniques," 2017 Recent Developments in Control, Automation & Power Engineering (RDCAPE), Noida, India, 2017, pp. 453-458, doi: 10.1109/RDCAPE.2017.8358314.
[11] J. Ding, G. Li, H. Zhang, A. Zhang and J. Huang, "A Novel DPS Control of Dual Active Bridge DC-DC Converters to Minimize Current Stress and Improve Transient Response," 2021 33rd Chinese Control and Decision Conference (CCDC), Kunming, China, 2021, pp. 2130-2135, doi: 10.1109/CCDC52312.2021.9601547.
[12] A. Vetrivelan, W. Xu, R. Yu and A. Q. Huang, "Triple Phase-Shift Optimization of SiC-based Dual-Active Bridge DC/AC Converter," 2022 IEEE Applied Power Electronics Conference and Exposition (APEC), Houston, TX, USA, 2022, pp. 70-77, doi: 10.1109/APEC43599.2022.9773574.
[13] Gierczynski, M.; Grzesiak, L.M.; Kaszewski, A. Cascaded Voltage and Current Control for a Dual Active Bridge Converter with Current Filters. Energies 2021, 14, 6214. https://doi.org/10.3390/en14196214
[14] Z. Yu, J. Zeng, J. Liu and F. Luo, "Terminal sliding mode control for dual active bridge dc-dc converter with structure of voltage and current double closed loop," 2018 Australian & New Zealand Control Conference (ANZCC), 2018, pp. 11-15, doi: 10.1109/ANZCC.2018.8606608.
[15] Y. Ma, H. Wen, X. Zhou and J. Yin, "Modeling and Control Strategy Simulation of Dual Active Bridge DC-DC Converter," 2021 IEEE International Conference on Mechatronics and Automation (ICMA), 2021, pp. 431-435, doi: 10.1109/ICMA52036.2021.9512593.